

High resolution β -NMR study of $^8\text{Li}^+$ implanted in gold

T. J. Parolin,¹ Z. Salman,^{2,*} K. H. Chow,³ Q. Song,⁴ J. Valiani,¹ H. Saadaoui,⁴ A. O'Halloran,² M. D. Hossain,⁴ T. A. Keeler,⁴ R. F. Kiefl,^{2,4,5} S. R. Kreitzman,² C. D. P. Levy,² R. I. Miller,² G. D. Morris,² M. R. Pearson,² M. Smadella,⁴ D. Wang,⁴ M. Xu,² and W. A. MacFarlane¹

¹*Department of Chemistry, University of British Columbia, Vancouver, British Columbia, V6T 1Z1, Canada*

²*TRIUMF, 4004 Wesbrook Mall, Vancouver, British Columbia, V6T 2A3, Canada*

³*Department of Physics, University of Alberta, Edmonton, Alberta, T6G 2G7, Canada*

⁴*Department of Physics and Astronomy, University of British Columbia, Vancouver, British Columbia, V6T 1Z1, Canada*

⁵*Canadian Institute for Advanced Research, Toronto, Ontario, M5G 1Z8, Canada*

(Received 23 December 2007; revised manuscript received 20 May 2008; published 16 June 2008)

We report the behavior of low energy $^8\text{Li}^+$ implanted into gold as revealed by beta-detected NMR. At an external magnetic field of 3 T, two narrow resonances are observed, which are attributed to Li in the octahedral interstitial and the substitutional lattice sites. The Knight shifts for these two resonances are found to be temperature independent with values of +141(4) and +73(5) ppm, respectively. The spin-lattice relaxation rate in high magnetic fields at 290 K is slow, consistent with the Korringa relation; however, the rate increases dramatically for magnetic fields below about 2 mT. We attribute this to interaction of the ^8Li spin with the host lattice nuclear spins.

DOI: [10.1103/PhysRevB.77.214107](https://doi.org/10.1103/PhysRevB.77.214107)

PACS number(s): 76.60.-k, 76.30.Lh, 75.70.Ak

I. INTRODUCTION

With the recent application of low energy beta-detected nuclear magnetic resonance (β -NMR) as a local probe of the electromagnetic properties of thin films, heterostructures, and near the surfaces of crystals,¹⁻⁷ it has become important to establish the detailed behavior of the probe nuclei (^8Li) in a variety of simple materials. In particular, in this work, we focus on the face-centered cubic (fcc) metal gold. Au is particularly interesting for its chemical inertness,⁸ which is the basis of its common use as a capping layer in many thin film heterostructures, protecting sensitive underlayers from oxidation. Its high density is especially significant here since low energy ions can be implanted in very thin Au overlayers.⁷ For instance, it may be possible to study the magnetization of a buried interface by implanting the probe ions into a thin Au overlayer and perform the investigation proximally.⁹ In such an experiment, the magnetization of the interface or underlayer would perturb the magnetic field in the capping layer, causing a broadening and possibly a shift of the resonance. It is thus an important prerequisite for such studies (and the topic of this work) to establish the behavior of the probe in the unperturbed Au host.

Here we report results of β -NMR studies of ^8Li in bulk Au. At high external magnetic field, we find two well-resolved resonances, with temperature-dependent amplitudes that correspond to different cubic stopping sites for the ^8Li . A site change transition, apparent in a crossover of the resonance amplitudes, occurs centered at about 190 K. We make an accurate measure of the small positive Knight shifts of these lines: +73(5) and +141(4) ppm. At 290 K the spin-lattice relaxation rate ($1/T_1$) is correspondingly slow, but for very low magnetic fields (<2 mT) the relaxation increases as the ^8Li begins to interact with the dynamic nuclear spins of the host lattice. By varying the implantation energy, we find no significant depth dependence of the resonances.

II. EXPERIMENT

The experiments were conducted at the TRIUMF ISAC facility, which provides a low energy (~ 30 keV) beam of hyperpolarized¹⁰ $^8\text{Li}^+$ with a typical rate of $10^6/\text{s}$. Here, we briefly describe the β -NMR technique as implemented at TRIUMF; additional technical details may be found in Refs. 11 and 12.

The probe ^8Li has spin $I=2$, nuclear gyromagnetic ratio $\gamma=6.3015$ MHz/T, lifetime $\tau=1.21$ s, and small quadrupole moment $Q/e=+31$ mb. A high degree of spin polarization of the ^8Li probe nuclei is produced in-flight by optical pumping.¹³ By selecting the sense of circular polarization (helicity) of the pumping laser, one can select the spin polarization direction to be either parallel or antiparallel to the applied magnetic field. Data is collected under both polarizations alternately for accurate baseline determination. The $^8\text{Li}^+$ are implanted into the sample mounted on a helium coldfinger cryostat (3–310 K), in an ultrahigh vacuum (UHV) chamber contained in the bore of a high homogeneity superconducting solenoid that produces a static longitudinal magnetic field H_0 along the beam direction. Typically, the beam is focused to a 3-mm diameter beamspot. The beta decay countrates are measured using two fast plastic scintillation counters located 180° opposite each other along the beam axis, in front of (forward, F), and behind (backward, B) the sample. The beam passes through a small aperture in the back counter. The asymmetry in the decay rates from the two counters $A=(F-B)/(F+B)$ is the experimentally measured quantity and is directly proportional to the ^8Li nuclear spin polarization.

To measure resonances, $^8\text{Li}^+$ is implanted continuously, and the time-averaged nuclear polarization is monitored as a function of the frequency ν of a small radio-frequency (RF) field H_1 applied transverse to the polarization by a transmission line Helmholtz coil. The frequency is stepped slowly on the scale of τ over a range around the resonance, correspond-

ing to many cycles of ν ; the resonances are thereby acquired using continuous-wave (CW) RF. On resonance, ν matches the Larmor frequency of ^8Li ($\nu_0 = \gamma H_0$), resulting in fast precession of the polarization around the direction of H_1 , reducing the time-averaged A . The observed resonance thus appears as a *decrease* in A . The amplitude of the RF field is monitored with a directional coupler and a calibrated power meter on the input of the (nonresonant) tank circuit, yielding the measured power P_{rf} . For this coil, $H_1[\mu\text{T}] \sim 13\sqrt{P_{rf}[\text{W}]}$. The frequency range is often scanned several times for both helicities. Prior to analysis, the scans of a given helicity are averaged, and the resulting two spectra are combined. Because the spin polarization is not generated by the applied field, and the signal is detected via the asymmetric β decay, the resonance signal-to-noise is *independent of frequency* ν , in contrast to the ν^2 dependence of conventional NMR. This enables experiments to be carried out easily over a wide range of applied magnetic fields.

The spin-lattice relaxation rate T_1^{-1} is measured by monitoring the time dependence of the nuclear polarization in the absence of the RF field. In the T_1 experiments, the incident ion beam is pulsed using a fast electrostatic kicker, and the loss of the initial nuclear polarization with time [i.e., $A(t)$] is measured after each pulse. A pulse length of 0.5 s duration, followed by a counting period of 10 s was used. Note that very few ^8Li survive more than the corresponding eight exponential lifetimes from the pulse. For this reason it is difficult to measure very slow ($T_1 \gg \tau$) relaxation accurately. Decay events are accumulated by repeating this cycle every 15 s. Like the resonance data, T_1^{-1} is measured using alternate helicities, which are subsequently combined for analysis. To extract a relaxation rate the asymmetry following the beam pulse is fit to a single exponential decay: $A(t) = A_0 e^{-t/T_1}$, where A_0 is the initial asymmetry.

To vary the implantation energy of the ion beam, the spectrometer can be biased with a high positive electrostatic potential, allowing the average implantation depth to be varied in the range 2–200 nm.

In this work we studied two samples of Au to verify that the results are intrinsic. Some preliminary results of the resonance behavior of ^8Li in a third sample are reported in Ref. 14. However, in that work no reference signal was available to measure the relative shifts, preventing a determination of the Knight shift, K . Here a Au film was deposited on a (100) MgO substrate, and we use the ^8Li resonance in the substrate as an *in-situ* frequency reference. This film (sample I) is 100 nm thick grown by thermal evaporation from a 99.99% pure source at a rate of ~ 4 Å/s under a background pressure of 10^{-6} torr. The thickness of the film was estimated using a calibrated thickness-rate monitor during deposition, and shows a preferred orientation along the (111) direction as determined by x-ray diffraction. Data is also presented for ^8Li implanted in a 25 μm 99.99% pure foil (Alfa Aesar), denoted as sample II.

III. RESULTS

A. Resonance spectra

The CW RF acquisition mode results in resonances that, for low P_{rf} , are Gaussian in shape, while at higher power, are

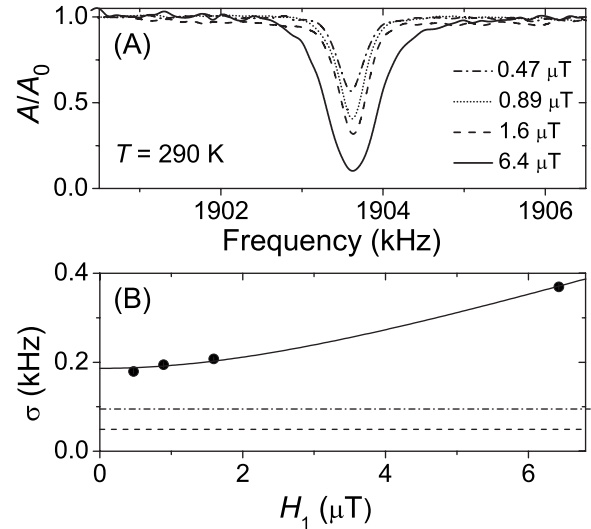


FIG. 1. (a) Spectra recorded in sample II at 0.3 T, 290 K, and 30.5 keV implantation energy as a function of the amplitude of the RF field, H_1 . (b) Gaussian [$\exp(-\nu - \nu_{\text{res}})^2 / 2\sigma^2$] linewidths σ of the spectra in (a). An intrinsic linewidth $\sigma_0 = 186(5)$ Hz due to the static host nuclear moments is obtained for $H_1 = 0$. The horizontal lines indicate the calculated, powder average, van Vleck linewidths for the undistorted O (dot-dash line) and S (dashed line) sites.

well described by power-broadened Lorentzian lineshapes. The linewidth (σ) depends on the amplitude of the RF field H_1 via

$$\sigma^2 = \lambda^2 + \sigma_0^2 + (\gamma H_1)^2, \quad (1)$$

where σ_0 is the intrinsic static linewidth, which, in the absence of other contributions, is just due to the distribution of host nuclear dipole fields at the probe site, i.e., the well-known van Vleck linewidth.¹⁵ The dynamic contribution is $\lambda = 1/\tau + 1/T_1$, which in Au, at all temperatures studied here, is at least 2 orders of magnitude smaller than σ_0 and can thus be neglected. At high P_{rf} , the last term in Eq. (1) dominates the width. The resonance also increases in *amplitude* with H_1 , eventually saturating when the ^8Li is completely depolarized. Figure 1 shows an example of the dependence of the resonance on H_1 in Au at $H_0 = 0.3$ T. Below about 30 mW (~ 2 μT), the width is the H_1 -independent intrinsic σ_0 . Practically, a compromise between broadening and amplitude is made to determine which RF power is used. High power may reveal broad lines that are undetectable at lower power but does not give an accurate measure of the intrinsic linewidth. The condition for detectability is that a significant fraction of the ^8Li spin polarization lies within the RF bandwidth (γH_1) on resonance. With the maximum $H_1 \sim 0.1$ mT, we can observe resonances as wide as 30 kHz FWHM.

At room temperature, in magnetic fields above ~ 1 T, the spectrum of ^8Li in Au exhibits a single narrow resonance near ν_0 . Figure 2 shows the resonance at 290 K in sample I. At this implantation energy (28 keV) only a small fraction of the ^8Li penetrate the Au film to stop in the MgO. The resonance from $^8\text{Li}^+$ in the MgO substrate is not shifted and thus provides a convenient measure of ν_0 ,⁹ allowing us to determine the relative frequency shift of the resonance in Au at

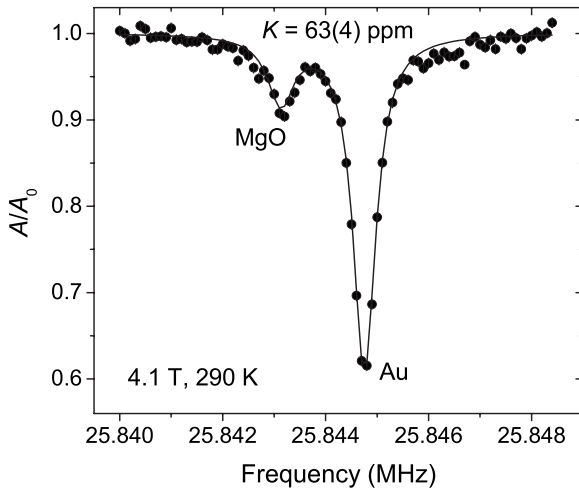


FIG. 2. A typical spectrum of $^8\text{Li}^+$ implanted into sample I at 28 keV for $H_1 \sim 3 \mu\text{T}$, showing the large resonance in Au and the smaller resonance in the MgO substrate. The spectrum is fitted with two Lorentzians (solid line).

290 K as $K = (\nu - \nu_0) / \nu_0 = +63(4)$ parts per million (ppm), where ν is the position of the peak corresponding to ^8Li in Au.

As the temperature T is lowered, a second resonance at slightly higher frequency appears and grows in intensity at the expense of the original.¹⁴ For example, Fig. 3 shows the temperature dependence of the spectra in sample II as a function of temperature. This is observed in several samples of Au, confirming that it is intrinsic to isolated ^8Li in Au. The second resonance is found at higher frequency upon cooling, at +131(4) ppm. The magnetic origin of the relative shifts was confirmed, for example, by reducing H_0 to 0.3 T where the two resonances are not resolved. As discussed in Sec. IV,

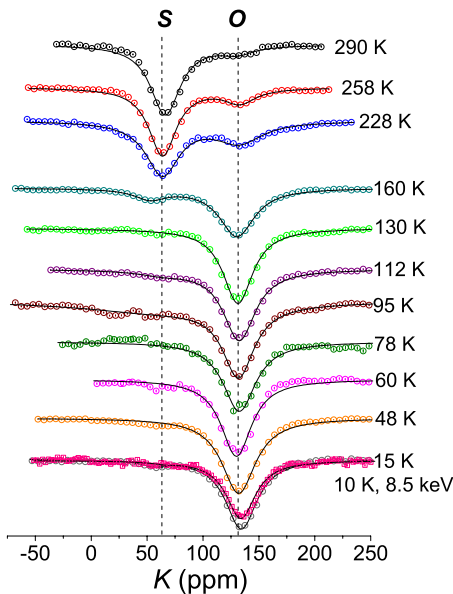


FIG. 3. (Color online). Resonance spectra recorded in sample II for $H_0=3 \text{ T}$ and $H_1 \sim 5 \mu\text{T}$ at 30.5 keV (circles), and at 8.5 keV at 10 K (squares). The solid lines are fits using one ($T < 150 \text{ K}$) or two Lorentzians ($T > 150 \text{ K}$).

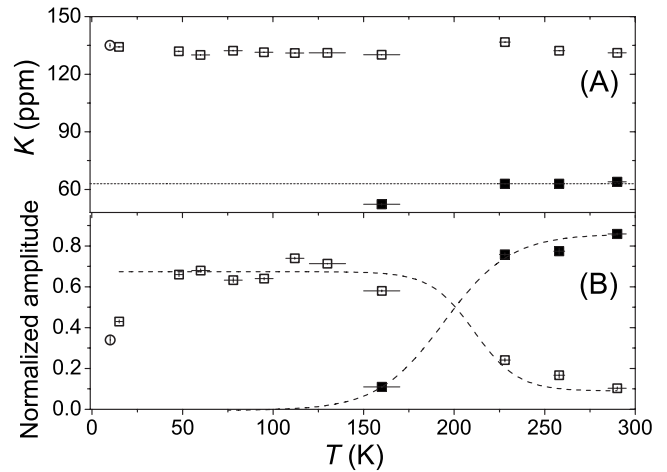


FIG. 4. Temperature dependence of (a) Knight shift and (b) the amplitudes of the 3 T resonances in sample II from the Lorentzian fits in Fig. 3. O site line, open symbols; S site line, filled symbols; 8.5 keV data, circles.

by analogy with the behavior of (i) the temperature dependence of the resonances and (ii) the relative sizes of the shifts in the other group 11 fcc metals,^{1,6} we provisionally assign the high frequency resonance to Li in the octahedral interstitial (O) site of the Au lattice, and the lower frequency line to the substitutional (S) site.

We find the high field spectra at $H_1 \sim 5 \mu\text{T}$ fit well to Lorentzian lineshapes. From such fits, the shifts and amplitudes are shown in Fig. 4. The shifts are independent of temperature (consistent with Knight shifts), while the amplitudes show a crossover at about 190 K, somewhat higher than a similar crossover in Ag.¹ As the temperature is further decreased (below 50 K) the amplitude of the narrow O resonance decreases [Fig. 4(b)]; a similar reduction of the O resonance is seen in Cu,⁶ but not in Ag.¹

To investigate the possibility of depth dependence of the resonances, we studied the spectra as a function of implantation energy for several energies ranging from 8.5 to 30.5 keV, corresponding to mean implantation depths in the range 25–70 nm, according to Monte Carlo simulations using TRIM.SP and SRIM2006.¹⁶ No significant depth dependence of the resonances was observed in either sample.

B. Spin-lattice relaxation

We turn now to measurements of the spin-lattice relaxation rate. Two examples of ^8Li relaxation spectra in samples I and II at 290 K are shown in Fig. 5. In both, $A(t)$ following the 0.5 s beam pulse is well described by a single exponential decay. Unlike conventional NMR, this type of T_1 measurement is not spectrally resolved, i.e., the measured rate corresponds to a weighted average over all stopping sites, which may differ in their relaxation rates. However, the data shows no indication of multiple relaxing components,¹⁷ consistent with the single (S site) resonance at this temperature. At 13 keV, the fraction of ions that penetrate the Au layer is negligible. The agreement between the two samples is quite good so we take the average, $T_1^{-1} = 0.127(7) \text{ s}^{-1}$, as the Korringa rate at this temperature.

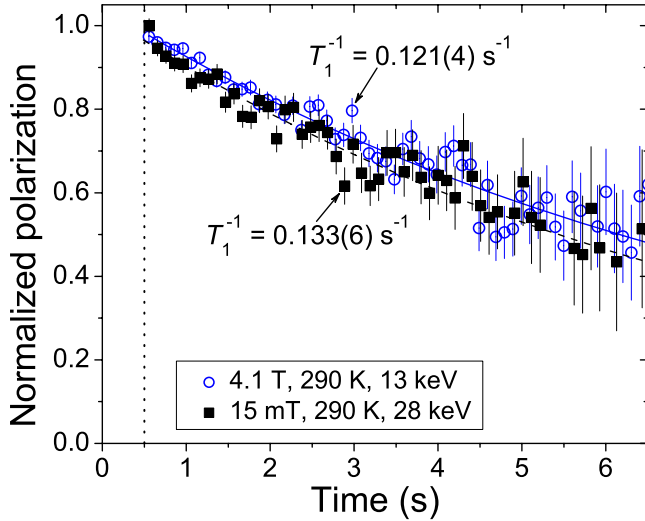


FIG. 5. (Color online). Spin-lattice relaxation spectra of ^8Li in sample I at 4.1 T (open circles; solid line) and sample II at 15 mT (filled squares; dashed line) at 290 K. The data are fit to a single exponential after a 0.5 s beam pulse, indicated by the vertical line.

The H_0 dependence of the relaxation rate at 290 K is shown in Fig. 6. It is independent of field down to about 2 mT, below which, it shows a marked increase. The amplitude A_0 is also significantly field dependent in this range, falling to about one third of its high field value as the field approaches zero (inset of Fig. 6). The field independence of $1/T_1$ at high field is consistent with the Korringa mechanism, i.e., spin-flip scattering of conduction electrons from the ^8Li nucleus. In conventional NMR of metals at low fields,¹⁸ the Korringa rate increases by a factor of 2. In contrast, we find a tenfold increase, suggesting that, instead, there is an additional relaxation mechanism operative at low field, i.e., a

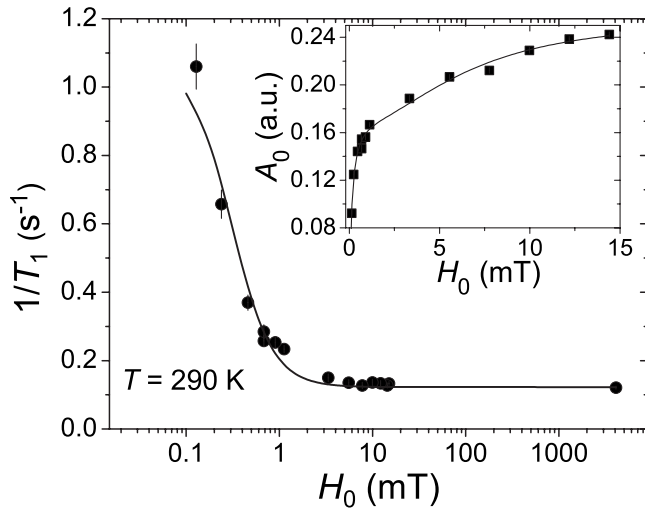


FIG. 6. Applied field dependence of the spin-lattice relaxation rate at 290 K in sample II at 28 keV implantation, except the point at 4.1 T, which is from sample I at 13 keV. The solid line is a fit to a Lorentzian. Inset: Initial asymmetry of the relaxing component as a function of applied field. Above 15 mT this value becomes field independent. The solid line is a guide to the eye.

zero crossing resonance,¹⁹ where at zero field the ^8Li and ^{197}Au Larmor frequencies coincide, enabling a resonant loss of ^8Li polarization to the host lattice nuclear spin bath. A similar increase is seen in the spin lattice relaxation of ^8Li in Cu at low field.²⁰ A Lorentzian of width 0.6(1) mT fits the field dependence of the rate reasonably well (Fig. 6). A more detailed study of the field and temperature dependence of the low field relaxation is the subject of a future report.

IV. DISCUSSION

We begin by pointing out the similarity in the temperature dependence of the resonances of $^8\text{Li}^+$ implanted in Au and Ag.¹ In both metals, at high field, two narrow resonances slightly positively shifted from the Larmor frequency with nearly T -independent positions, but strongly T -dependent amplitudes are observed. This is also found for ^8Li in Cu, but in Cu the resonances are not well resolved.⁶ The absence of quadrupolar splitting of the resonances implies that the ^8Li site has cubic symmetry. Recall the quadrupolar interaction couples the nuclear spin to the local electric field gradient (EFG), and the EFG is identically zero for sites of cubic symmetry. There are only three cubic sites in the fcc lattice, namely the substitutional (S), the octahedral (O), and tetrahedral (T) interstitials. The resonance frequencies of these sites will be distinguished by differing hyperfine couplings to the Au conduction electrons, yielding different Knight shifts. Thus we suppose the observed resonances correspond to two of these three possible sites. Provisionally we assign the high temperature line to the most spacious of the three, the S site, and the low temperature line to the next largest, the O site. These assignments are consistent with β -NMR measurements²¹ and calculations²² for ^8Li in isostructural Ni, as well as alpha particle channeling results.²³ They are also in agreement with β -NMR cross-relaxation results for a different implanted probe, ^{12}B , in Cu.^{24,25} Definitive site determinations may be possible with similar cross-relaxation measurements on ^8Li in, e.g., Cu.²⁰ In this scenario, the temperature-dependent resonance amplitudes result from a thermally activated ($O \rightarrow S$) site change, i.e., Li in the smaller O site is metastable. This is reasonable, since occupation of a larger site should correspond to a lower energy configuration for the implanted Li. For T above ≈ 150 K, the Li has sufficient thermal energy to migrate to a nearby vacancy and become substitutional. The vacancy is likely not thermal in origin, but rather a product of the Li implantation itself.²⁶

The dipolar linewidth is also site dependent, but uncertainty in the extent of local lattice distortion around the implanted ^8Li makes it difficult to use conclusively for determining the site. However, such calculations are in reasonable agreement^{27,28} with the assignments for light beta-active ions implanted in Cu. Because of the small ^{197}Au nuclear moment, we expect small dipolar widths. Indeed, it is only because the lines are so narrow that we can resolve such closely spaced resonances, in contrast to Cu.⁶ The widths of the ^8Li resonances in Au exceed the dipolar (van Vleck) widths calculated for the undistorted lattice. For the O and S sites, the calculated powder average widths are 95 Hz, and

TABLE I. Summary of β -NMR shifts K , hyperfine couplings A_{hf} , and Korringa ratios \mathcal{K} for $^8\text{Li}^+$ in the group 11 metals, Cu (Ref. 6), Ag (Ref. 1), and Au (this work). The Korringa ratio from conventional NMR \mathcal{K}_{NMR} from Ref. 32 is also shown for comparison.

Host	K^c (ppm)		A_{hf} (kG/ μ_B)		A_{hf}^O/A_{hf}^S	\mathcal{K} S site	\mathcal{K}_{NMR}
	S	O	S	O			
Cu	+136(3)	+197(3)	4.8(1)	13.8(2)	2.9(1)	1.46(4)	1.83(15)
Ag	+128(13)	+220(16)	6.2(6)	21(2)	3.4(5)	1.44(2)	2.22(20)
Au	+73(5)	+141(4)	2.8(2)	10.7(3)	3.8(3)	1.01(6)	1.40(16)

49 Hz, respectively [horizontal lines in Fig. 1(b)]. The origin of the additional linewidth is not clear. The widths from the fits in Figs. 2 and 3 show no temperature dependence and are similar for both S and O resonances; thus, they are not due to residual (ppm level) magnetic impurities in the Au, which would yield a temperature- and field-dependent width. The broadening may simply arise from a local contraction of the Au lattice about the ^8Li , decreasing the distance to the near neighboring Au dipoles and increasing the van Vleck width. This possibility has been reported for other implanted probes, e.g., negatively charged muonium in n -type GaAs,²⁹ and ^{12}B in ZnSe.³⁰ Alternatively, the linewidth may reflect a narrow, unresolved quadrupolar powder pattern if the ^8Li site is not perfectly cubic. Slightly noncubic sites could result from a small symmetry-breaking local lattice distortion caused by the ^8Li or, as has been suggested for ^{12}B in Cu and Al,²⁸ the occurrence of distant point defects created by the ^8Li implantation. For the remainder of this discussion, we will assume our site assignment is correct, noting that most of the comparisons will not be altered greatly if an alternate subset of the three cubic sites is chosen, the main difference being the site coordination n .

K is taken to be a site-dependent Knight shift that arises from a coupling of the ^8Li to the small, T -independent Pauli susceptibility of the host χ_P . However, the raw shift contains a contribution due to demagnetization.⁹ For films and thin foils, the demagnetization factor N is very close to 4π , and the corrected shift K^c is obtained by adding $\Delta k = 2N\chi_P/3$ to the measured K . Using $\chi_P = 1.21 \times 10^{-6}$ emu/cm³ (Ref. 31) yields the corrected shifts $K_O^c = +141(4)$ ppm and $K_S^c = +73(5)$ ppm. The ratio of the shifts for the two sites is then $K_O^c/K_S^c \sim 2$, corresponding to a splitting of 68(6) ppm, and the shifts are independent of T in the range 10–290 K [Fig. 4(a)]. The splitting between the S and O lines observed in the polycrystalline Au foil (sample II) is the same as that measured in more highly oriented films (sample I and a 50 nm film¹⁴), indicating that K , and thus A_{hf} , is predominantly isotropic, as expected for a cubic host.

The site dependence is attributed to differing hyperfine coupling constants A_{hf} , resulting from hybridization of the $^8\text{Li}^+$ $2s$ orbital with the Au conduction band. A_{hf} is typically expressed in units of kG/ μ_B , where μ_B is the Bohr magneton, and is given by

$$A_{hf} = \frac{K^c N_A \mu_e}{n \chi_P}, \quad (2)$$

where N_A is Avogadro's number, n is the coordination number of the site (12 for S ; 6 for O), and μ_e is the electron

magnetic moment (9.28×10^{-24} J/T). Using Eq. (2), $A_{hf}^S = 2.8(2)$ kG/ μ_B and $A_{hf}^O = 10.7(3)$ kG/ μ_B .

These values are compared to those for ^8Li in the other group 11 metals in Table I. For a given site, the coupling constants vary by no more than a factor of 2 in these metals. The origin of the difference in A_{hf} between different hosts is a complex question that requires careful consideration of several factors such as the band structure of the host, the local electronic structure of the $^8\text{Li}^+$ defect (including screening), and the local structural relaxation around the implanted ion. The latter is particularly important for interstitial (O) ions.^{22,33} A_{hf} depends in part on the strength of the hybridization, which in the simplest picture is a function of n and the distance between the probe and the neighboring host atoms. Comparing the O site to the S site, n is half as large, but the distance to the nearest-neighbors is less. If this was the only consideration, one would then expect similar A_{hf} s for Au and Ag as the lattice constants for these metals are essentially equal, instead the coupling constants for Au are about half the values for Ag (and χ_P for these two metals differs by only 22%). The energy of the screened $^8\text{Li}^+$ $2s$ state with respect to the host Fermi level will also be important in determining A_{hf} . Table I also lists the ratio A_{hf}^O/A_{hf}^S , which is found to be similar for all three metals although it is slightly larger for Au and Ag than Cu, in accordance with the trend in lattice constants. We find that the lower coordination site (O) experiences a larger hyperfine field than the higher coordination site (S) in all three hosts. This is not likely universal, however, as calculations for various implanted impurities predict the opposite may occur, especially for ferromagnetic hosts like Fe or Ni.^{33,34} Thus, hyperfine fields are very sensitive to the identity of both the impurity atom and the host. First-principles calculations are needed to understand the subtleties involved for a given system. Such calculations are beyond the scope of this work but would provide stringent tests of electronic structure models, that up to now have mainly focused on impurities implanted in magnetic hosts where the fields are large. Similar calculations for nonmagnetic defects in nonmagnetic hosts, such as ^8Li in Au, would be interesting to compare to our measurements.

At high fields, where the electron-nuclear (Korringa) mechanism is dominant, the spin-lattice relaxation rate of ^8Li , at room temperature, in both Ag (Ref. 1) and Cu (Ref. 6) is nearly 3 times faster than in Au. The present, averaged room temperature relaxation time in Au (Fig. 5), $T_1 = 7.9(4)$ s, is half the 17(3) s reported by Koenig *et al.*,³⁵ but double the 4(1) s measured by Haskell and Madansky.³⁶ Thus, our result is within the range of the two reported times,

but the origin of the discrepancy is not certain, especially since the previous results differ from each other by a factor of 4. It is noted that all three times were obtained for $H_0 > 2$ mT, where we have determined T_1^{-1} to be field independent (Fig. 6). The authors of Ref. 35 note that in both of the previous studies (using MeV recoil ions) the temperature of the Au samples was not controlled during irradiation; however, they conclude that contamination of the sample surface was the most likely reason for the faster 4(1) s relaxation time reported in the earliest study. A relaxation time of 3.3(3) s is also reported in Ref. 35 for ^8Li in Ag foil at room T , which agrees very well with measurements by our group for ^8Li in a Ag film.¹ We note that the determination of relaxation times that are significantly longer than the radioactive lifetime of the probe τ is difficult. Our method, using both parallel and antiparallel spin polarization, accurately determines the baseline corresponding to the thermal equilibrium polarization, even though the relaxation is too slow to approach this value during the experiment. Combined with the sample independence evident in Fig. 5, we conclude our measurement is the most reliable measurement to date.

The Korringa law relates the relaxation rate to the square of the Knight shift.^{15,31} As a consequence, the Korringa ratio,

$$\mathcal{K} = (K^c)^2 T_1 T / S, \quad (3)$$

where S is a nucleus-specific constant that for ^8Li is equal to 1.20×10^{-5} sK. \mathcal{K} is a dimensionless constant equal to 1 in the limit of noninteracting conduction electrons. Conduction electron correlations cause \mathcal{K} to deviate from unity, with disorder playing an important role.³⁷ \mathcal{K} is thus often used as a phenomenological measure of conduction electron correlations, but even for rather weakly interacting electrons, it often exceeds unity.¹⁵ By combining our averaged T_1^{-1} value with K^c in Eq. (3), we obtain $\mathcal{K} = 1.01(6)$ for ^8Li in Au at 290 K, remarkably close to the ideal value and very different from in the strongly ferromagnetically correlated metal, Pd (cf. Ref. 2).

The \mathcal{K} values for the S site in the other group 11 hosts are given in Table I. They reveal an enhancement for ^8Li in Ag and Cu, which is the same within error; however, conventional NMR (conducted at cryogenic temperatures to improve signal-to-noise)³² give a slightly larger \mathcal{K} for Ag than Cu, but a value for Au that is less than either Ag or Cu. A smaller Korringa ratio for ^8Li in Au, thus, seems consistent. However, the value obtained from conventional NMR in Au³² is somewhat larger [$\mathcal{K} = 1.4(2)$]. Substitutional ^8Li should have approximately the same hyperfine form factor [i.e., the spatial Fourier transform of the hyperfine coupling $A_{hf}(q)$, where q is the wave vector] as the intrinsic Au, so the difference in \mathcal{K} is not likely a result of a different filtering effect of $A_{hf}(q)$ on finite wavelength conduction electron correlations. Rather the presence of the $^8\text{Li}^+$ itself may renormalize \mathcal{K} via scattering.

The sum of the normalized (divided by the initial baseline asymmetry A_0) amplitudes in Fig. 4(b) for temperatures

above the site transition is almost 1, indicating that the resonance is *nearly* saturated [cf. Fig. 1(a)]. Below the transition, however, this is clearly not the case and, in particular, the $\sim 40\%$ decrease in normalized amplitude below 50 K suggests that there is an unresolved signal that is too broad to be observed at the P_{rf} of Fig. 3. This is similar to what has been reported for ^8Li in Cu.⁶ Indeed, the spectra from ^8Li in a 50 nm Au film¹⁴ exhibit an asymmetric broadening at low temperatures; however, H_1 in those measurements was an order of magnitude larger than that used in the present work. The narrow lines (with widths in the range of static dipolar values) correspond to ^8Li in well-defined cubic sites in the host lattice; thus, this broad component must coexist with the cubic O site, and it is only observable at high H_1 . Such a broadening could be quadrupolar due to implantation-related defects, which at low temperature are near the ^8Li stopping site. The appearance of a “disordered site” below 50 K is consistent with the quasicontinuous recombination of correlated vacancy-interstitial (Frenkel) pairs in this temperature range due to the high mobility of the Au self-interstitial.³⁸ We note such low temperature broadening (at large H_1) or the resulting reduced signal amplitude (at small H_1) is not seen for ^8Li in Ag.¹

V. CONCLUSIONS

To summarize, we have studied the β -NMR of low energy ^8Li implanted in bulk Au. We find narrow resonances corresponding to two cubic Li sites, provisionally assigned to ions in the octahedral interstitial O and substitutional S sites. We find a site transition from the metastable O site to the S site centered at about 190 K. We find no evidence for depth dependence of the resonances for the implantation range studied. At low RF power, the spectra in Au are very similar to those in Ag, but with smaller shifts and a correspondingly slower spin-lattice relaxation rate. The latter is found to be highly field dependent for external magnetic fields less than 2 mT.

The broad resonance seen below 50 K at high P_{rf} (Ref. 14) is not detected at the small H_1 used here, making low temperature proximal magnetometry⁹ using ^8Li implanted in a Au capping layer feasible, though not as simple as in Ag. However, the advantages of Au (higher density, lower reactivity, and the tendency to form flatter films³⁹) make it an important candidate for this application. This study establishes the basic behavior of ^8Li in Au necessary for future β -NMR studies of thinner Au films and capping layers.

ACKNOWLEDGMENTS

We thank A. Kulpa for growing the Au/MgO film. We acknowledge the technical assistance of R. Abasalti, B. Hitti, D. Arseneau, S. Daviel, and funding from NSERC. TRIUMF is funded in part by NRC (Canada).

- *Present address: Clarendon Laboratory, Department of Physics, Oxford University, Parks Road, Oxford OX1 3PU, UK.
- ¹G. D. Morris, W. A. MacFarlane, K. H. Chow, Z. Salman, D. J. Arseneau, S. Daviel, A. Hatakeyama, S. R. Kreitzman, C. D. P. Levy, R. Poutissou, R. H. Heffner, J. E. Elenewski, L. H. Greene, and R. H. Kiefl, *Phys. Rev. Lett.* **93**, 157601 (2004).
 - ²T. J. Parolin, Z. Salman, J. Chakhalian, Q. Song, K. H. Chow, M. D. Hossain, T. A. Keeler, R. F. Kiefl, S. R. Kreitzman, C. D. P. Levy, R. I. Miller, G. D. Morris, M. R. Pearson, H. Saadaoui, D. Wang, and W. A. MacFarlane, *Phys. Rev. Lett.* **98**, 047601 (2007).
 - ³Z. Salman, K. H. Chow, R. I. Miller, A. Morello, T. J. Parolin, M. D. Hossain, T. A. Keeler, C. D. P. Levy, W. A. MacFarlane, G. D. Morris, H. Saadaoui, D. Wang, R. Sessoli, G. G. Condorelli, and R. F. Kiefl, *Nano Lett.* **7**, 1551 (2007).
 - ⁴Z. Salman, D. Wang, K. H. Chow, M. D. Hossain, S. R. Kreitzman, T. A. Keeler, C. D. P. Levy, W. A. MacFarlane, R. I. Miller, G. D. Morris, T. J. Parolin, H. Saadaoui, M. Smadella, and R. F. Kiefl, *Phys. Rev. Lett.* **98**, 167001 (2007).
 - ⁵Z. Salman, R. F. Kiefl, K. H. Chow, M. D. Hossain, T. A. Keeler, S. R. Kreitzman, C. D. P. Levy, R. I. Miller, T. J. Parolin, M. R. Pearson, H. Saadaoui, J. D. Schultz, M. Smadella, D. Wang, and W. A. MacFarlane, *Phys. Rev. Lett.* **96**, 147601 (2006).
 - ⁶Z. Salman, A. I. Mansour, K. H. Chow, M. Beaudoin, I. Fan, J. Jung, T. A. Keeler, R. F. Kiefl, C. D. P. Levy, R. C. Ma, G. D. Morris, T. J. Parolin, D. Wang, and W. A. MacFarlane, *Phys. Rev. B* **75**, 073405 (2007).
 - ⁷T. A. Keeler, Z. Salman, K. H. Chow, B. Heinrich, M. D. Hossain, B. Kardasz, R. F. Kiefl, S. R. Kreitzman, W. A. MacFarlane, O. Mosendz, T. J. Parolin, and D. Wang, *Physica B* **374-375**, 79 (2006); T. A. Keeler, Z. Salman, K. H. Chow, B. Heinrich, M. D. Hossain, B. Kardasz, R. F. Kiefl, S. R. Kreitzman, C. D. P. Levy, W. A. MacFarlane, O. Mosendz, T. J. Parolin, M. R. Pearson, and D. Wang, *Phys. Rev. B* **77**, 144429 (2008).
 - ⁸See, e.g., B. Hammer and J. K. Nørskov, *Nature (London)* **376**, 238 (1995).
 - ⁹M. Xu, M. D. Hossain, H. Saadaoui, T. J. Parolin, K. H. Chow, T. A. Keeler, R. F. Kiefl, G. D. Morris, Z. Salman, Q. Song, D. Wang, and W. A. MacFarlane, *J. Magn. Reson.* **191**, 47 (2008).
 - ¹⁰Hyperpolarized nuclear spins have a population of the magnetic sublevels that is far from the Boltzmann distribution given by the Zeeman splitting at H_0 and the temperature. In the extreme limit, they would have 100% population in one of the $m = \pm l$ sublevels, i.e., for ^8Li , $m = \pm 2$.
 - ¹¹R. F. Kiefl, W. A. MacFarlane, G. D. Morris, P. Amaudruz, D. Arseneau, H. Azumi, R. Baartman, T. R. Beals, J. Behr, C. Bommas, J. H. Brewer, K. H. Chow, E. Dumont, S. R. Dunsiger, S. Daviel, L. Greene, A. Hatakeyama, R. H. Heffner, Y. Hirayama, B. Hitti, S. R. Kreitzman, C. D. P. Levy, R. I. Miller, M. Olivo, and R. Poutissou, *Physica B* **326**, 189 (2003).
 - ¹²Z. Salman, E. P. Reynard, W. A. MacFarlane, K. H. Chow, J. Chakhalian, S. Kreitzman, S. Daviel, C. D. P. Levy, R. Poutissou, and R. F. Kiefl, *Phys. Rev. B* **70**, 104404 (2004).
 - ¹³C. D. P. Levy, A. Hatakeyama, Y. Hirayama, R. F. Kiefl, R. Baartman, J. A. Behr, H. Izumi, D. Melconian, G. D. Morris, R. Nussbaumer, M. Olivo, M. Pearson, R. Poutissou, and G. W. Wight, *Nucl. Instrum. Methods Phys. Res. B* **204**, 689 (2003).
 - ¹⁴W. A. MacFarlane, G. D. Morris, T. R. Beals, K. H. Chow, R. A. Baartman, S. Daviel, S. R. Dunsiger, A. Hatakeyama, S. R. Kreitzman, C. D. P. Levy, R. I. Miller, K. M. Nichol, R. Poutissou, and R. F. Kiefl, *Physica B* **326**, 213 (2003).
 - ¹⁵C. P. Slichter, *Principles of Magnetic Resonance*, 3rd ed. (Springer-Verlag, Berlin, 1990).
 - ¹⁶W. Eckstein, *Computer Simulation of Ion-Solid Interactions* (Springer, Berlin, 1991); J. F. Ziegler, J. P. Biersack, and U. Littmark, *The Stopping and Range of Ions in Solids* (Pergamon, New York, 1984); SRIM2006 is available at <http://www.srim.org/>.
 - ¹⁷See, e.g., B. Bader, P. Heitjans, H.-J. Stöckmann, H. Ackermann, W. Buttler, P. Freilander, G. Kiese, C. van der Marel, and A. Schirmer, *J. Phys.: Condens. Matter* **4**, 4779 (1992).
 - ¹⁸A. G. Redfield, *IBM J. Res. Dev.* **1**, 19 (1957); A. G. Anderson and A. G. Redfield, *Phys. Rev.* **116**, 583 (1959); R. E. Walstedt, M. W. Dowley, E. L. Hahn, and C. Froidevaux, *ibid.* **138**, A1096 (1965); P. A. Fedders, *Phys. Rev. B* **13**, 4678 (1976).
 - ¹⁹See, e.g., B. E. Schultz, I. Fan, B. Hitti, R. F. Kiefl, and K. H. Chow, *Physica B* **374-375**, 464 (2006).
 - ²⁰A. I. Mansour, G. D. Morris, Z. Salman, K. H. Chow, T. Dunlop, J. Jung, I. Fan, W. A. MacFarlane, R. F. Kiefl, T. J. Parolin, H. Saadaoui, D. Wang, M. D. Hossain, Q. Song, M. Smadella, O. Mosendz, B. Kardasz, and B. Heinrich, *Physica B* **401-402**, 662 (2007).
 - ²¹Y. Nojiri, K. Ishiga, T. Onishi, M. Sasaki, F. Ohsumi, T. Kawa, M. Mihara, M. Fukuda, K. Matsuta, and T. Minamisono, *Hyperfine Interact.* **120-121**, 415 (1999).
 - ²²H. Fukuda and H. Akai, *J. Phys. Soc. Jpn.* **70**, 2019 (2001).
 - ²³H. Hofsäuss and G. Lindner, *Phys. Rep.* **201**, 121 (1991).
 - ²⁴E. Jäger, B. Ittermann, H.-J. Stöckmann, K. Bürkman, B. Fischer, H.-P. Frank, G. Sulzer, H. Ackermann, and P. Heitjans, *Phys. Lett. A* **123**, 39 (1987).
 - ²⁵B. Ittermann, H. Ackermann, H.-J. Stöckmann, K.-H. Erzevinger, M. Heemeier, F. Kroll, F. Mai, K. Marbach, D. Peters, and G. Sulzer, *Phys. Rev. Lett.* **77**, 4784 (1996).
 - ²⁶P. Ehrhart and H. Schultz, in *Atomic Defects in Metals*, edited by H. Ullmaier, Landolt-Börnstein, New Series, Group III Vol. 25: Condensed Matter (Springer-Verlag, Heidelberg, 1991), Chap. 2.
 - ²⁷F. Ohsumi, K. Matsuta, M. Mihara, T. Onishi, T. Miyake, M. Sasaki, K. Sato, C. Ha, A. Morishita, T. Fujio, Y. Kobayashi, M. Fukuda, and T. Minamisono, *Hyperfine Interact.* **120-121**, 419 (1999).
 - ²⁸T. K. McNab and R. E. McDonald, *Phys. Rev. B* **13**, 34 (1976).
 - ²⁹K. H. Chow, R. F. Kiefl, W. A. MacFarlane, J. W. Schneider, D. W. Cooke, M. Leon, M. Paciotti, T. L. Estle, B. Hitti, R. L. Lichti, S. F. J. Cox, C. Schwab, E. A. Davis, A. Morrobel-Sosa, and L. Zavieh, *Phys. Rev. B* **51**, 14762 (1995); K. H. Chow, B. Hitti, and R. F. Kiefl, in *Identification of Defects in Semiconductors*, edited by M. Stavola, Semiconductors and Semimetals Vol. 51A (Academic, New York, 1998), p. 137.
 - ³⁰B. Ittermann, G. Welker, F. Kroll, F. Mai, K. Marbach, and D. Peters, *Phys. Rev. B* **59**, 2700 (1999).
 - ³¹G. C. Carter, L. H. Bennett, and D. J. Kahan, in *Metallic Shifts in NMR*, edited by B. Chalmers, J. W. Christian, and T. B. Massalski, Progress in Materials Science Vol. 20 (Pergamon, Oxford, 1977), Pt. 1.
 - ³²A. Narath and H. T. Weaver, *Phys. Rev.* **175**, 373 (1968).
 - ³³H. Akai, M. Akai, S. Blügel, B. Drittler, H. Ebert, K. Terakura, R. Zeller, and P. H. Dederichs, *Prog. Theor. Phys.* **101**, 11 (1990).
 - ³⁴V. Bellini, S. Cottenier, M. Çakmak, F. Manghi, and M. Rots, *Phys. Rev. B* **70**, 155419 (2004).

- ³⁵I. Koenig, D. Fick, S. Kossionides, P. Egelhof, K.-H. Möbius, and E. Steffens, *Z. Phys. A* **318**, 135 (1984).
- ³⁶R. C. Haskell and L. Madansky, *Phys. Rev. C* **7**, 1277 (1973).
- ³⁷B. S. Shastry and E. Abrahams, *Phys. Rev. Lett.* **72**, 1933 (1994).
- ³⁸J. B. Ward and J. W. Kauffman, *Phys. Rev.* **123**, 90 (1961); F. W. Wiffen, C. L. Snead, Jr., and J. W. Kauffman, *Phys. Status Solidi* **32**, 459 (1969).
- ³⁹A. J. Francis and P. A. Salvador, *J. Mater. Res.* **22**, 89 (2007).